Published in final edited form as:
AJNR Am J Neuroradiol. 2016 May ; 37(5): 811–817. doi:10.3174/ajnr.A4623.

Mitotic activity in Glioblastoma correlates with estimated extravascular extracellular space derived from DCE-MRI

SJ Mills[1,2], **D du Plessis**[3], **P Pal**[3], **G Thompson**[1,2], **G Buonacorrsi**[2], **C Soh**[1,2], **GJM Parker**[2], and **A Jackson**[1,2]

[1]Department of Neuroradiology, Salford NHS Foundation Trust, Salford, U.K.

[2]Imaging Science and Biomedical Engineering, University of Manchester, U.K.

[3]Department of Neuropathology, Salford NHS Foundation Trust, Salford, U.K.

Abstract

Purpose—A number of parameters derived from dynamic contrast enhanced MRI (DCE-MRI) and separate histological features have been identified as potential prognosticators in high-grade glioma. This study evaluates the relationships between DCE-MRI derived parameters and histological features in glioblastoma multiforme (GBM).

Methods—28 patients with newly presenting GBM underwent pre-operative imaging (conventional imaging and T_1-DCE-MRI). Parametric maps of $IAUC_{60}$ (initial area under the contrast agent concentration curve), K^{trans} (contrast transfer co-efficient) v_e (estimate of volume of the extravascular extracellular space) and v_p (estimate of blood plasma volume) were generated and EnF was calculated. Surgical specimens were used to assess subtype and graded (WHO classification system) and assessed for necrosis, cell density, cellular atypia, mitotic activity and overall vascularity scores. Quantitative assessment of endothelial surface area, vascular surface area and a vascular profile count were made using CD34 immunostaining. The relationships between MRI parameters and histo-pathological features were examined.

Results—High values of K^{trans} were associated with the presence of frank necrosis (p=0.005). High values of v_e were associated with a fibrillary histological pattern (p<0.01) and with increased mitotic activity (p<0.05). No relationship was found between mitotic activity and histological pattern suggesting the correlation between v_e and mitotic activity was independent of histological pattern.

Conclusion—A correlation between v_e and mitotic activity is reported. Further work is warranted to establish how DCE-MRI parameters relate to more quantitative histological measurements including markers of proliferation and measures of vascular endothelial growth factor (VEGF) expression.

Corresponding Author Dr. Samantha Mills, Consultant Neuroradiologist, The Walton Centre, Fazakerley, Liverpool, L9 7LJ. Tel no. +44 151 525 3611. Samantha.Mills@thewaltoncentre.nhs.uk.

Conflict of Interest
None

Europe PMC Funders Author Manuscripts

Introduction

Gliomas are the commonest primary cerebral tumour of adulthood. They are histologically classified according to the World Health Organisation (WHO) criteria into tumour grade and subtype (1), which is important for determining appropriate treatment. Within given histological subtypes and tumour grades, a number of additional descriptive histopathological features have been identified as prognosticators including mitotic activity (2-4), microvascular density (MVD) (5,6) and certain vascular patterns (7,8). Both proliferation markers, such as Ki-67 (2-4,7,9,10) and expression of vascular endothelial growth factor (VEGF) (3,5,11-14) have also shown relationships to survival.

Dynamic contrast enhanced-MRI (DCE-MRI) techniques generate a number of parameters that characterize the microvascular environment. The enhancing fraction (EnF) describes the proportion of perfused tumour tissue. CBV and CBF are commonly derived from dynamic susceptibility contrast (DSC-MRI) techniques whilst volume transfer coefficient (K^{trans}), v_e (fractional volume of the extravascular extracellular space, EES) and v_p (fractional blood plasma volume) can be calculated from T_1-weighted DCE-MRI (15). In glioma, K^{trans}, v_p, EnF, CBV and CBF have been shown to relate to histological grade and/or subtype of tumour (16-21). In addition, K^{trans}, EnF and CBV have been identified as potentially grade independent prognosticators (22-25). The number of studies examining the relationship between DCE-MRI parameters and more specific histopathological features in glioma is currently small and predominantly focuses on vascular metrics such as blood volume and flow; however, significant correlations have been described between CBV and MVD (26-29), VEGF expression (27,30), cell density (29), endothelial proliferation (31) and mitotic activity (31) and between CBF and endothelial hyperplasia (32).

More recent studies have focused on the potential of v_e as an imaging biomarker. In glioma, it has shown value in discriminating between histological grade (33,34), but when compared with other potential candidate biomarkers of the extravascular extracellular space volume (Apparent Diffusion Co-efficient, ADC), on a voxel by voxel basis, no correlation was seen between the two metrics, suggesting that these parameters provide independent information about extravascular extracellular space characteristics (35). Two separate studies of glioma patients of various histological grade have both reported significant correlations between both K^{trans} and v_e and vascular and microvascular density (33,34), but neither study comments upon the relationship with cellular density or mitotic activity. A high field, 7T MRI study of rat xenografts showed an image matched significant negative correlation between v_e and tumor cellularity (36).

We hypothesized that: 1) larger, rapidly growing tumours would show higher mitotic activity as well as high angiogenic activity reflected by K^{trans} and EnF; and 2) more proliferative tumours would have a higher cellular density and mitotic activity associated with lower values of v_e.

Materials and Methods

Patients

Ethical approval was obtained and all patients gave informed consent. All tumours were histologically confirmed as GBM according to the WHO criteria (1). All imaging was pre-operative and patients received no treatment other than corticosteroids, which were administered for a minimum of 48 hours prior to imaging to allow stabilisation of the effects of steroids on DCE-MRI measures (37). Patients were excluded from the study if they had a history of renal dysfunction or low eGFR (<30 mls/min/1.73m^2).

MRI data acquisition

Imaging was performed on a 3 Tesla Philips Achieva system (Philips Healthcare, Best, Netherlands) using a SENSE head coil. DCE-MRI acquisitions were acquired in a sagittal oblique orientation to allow improved definition of the arterial input function (AIF) free from flow related artifact. Three pre-contrast T_1-fast field echo (T_1-FFE; RF-spoiled gradient echo) series (2°, 5°, 16°) were acquired for calculation of baseline T_1 maps (TR 3.5 ms, TE 1.1 ms, slice thickness 4.2 mm, 128 × 128 matrix, FOV 230 mm × 230 mm × 105 mm) in the same geometry. A dynamic, contrast-enhanced acquisition series (TR 3.5 ms, TE 1.1 ms, flip angle 16°, slice thickness 4.2 mm, 128 × 128 matrix, FOV 230 mm × 230 mm × 105 mm) consisting of 100 volumes with temporal spacing of approximately 3.4 seconds followed. A bolus dose of 0.1 mMolkg^{-1} (body weight) of gadolinium-based contrast agent (Gd-DTPA-BMA; Omniscan, GE Healthcare, Oslo, Norway) was injected at a rate of 3 mls^{-1}, after acquisition of the fifth image volume. Pre and post contrast T_1-weighted imaging sequences (TR 9.3 ms, TE 4.6 ms) were acquired in the same sagittal oblique geometry for definition of volume of interest (VOI) of the whole tumour.

MRI data analysis

An experienced neuroradiologist (SJM) manually defined VOIs for each tumour. The VOI corresponded to the enhancing tumour and all non-enhancing tissue contained within it on the post contrast T_1-weighted images. This technique has previously shown good interobserver agreement (Intraclass Correlation Coefficient > 0.94)(38). Pharmacokinetic analysis was performed on all pixels within the VOI which showed significant enhancement. Parametric maps of K^{trans}, v_p, v_e and $IAUC_{60}$ were produced using in-house software (MaDyM – Manchester Dynamic Modelling) and the extended Tofts and Kermode pharmacokinetic model (15). Automated AIFs were generated from an appropriately chosen slice, which included the internal carotid artery (39). Summary statistics for each parameter were generated for enhancing tumour tissue.

For each tumour, EnF ($EnF_{IAUC60>0}$) and thresholded EnF ($EnF_{IAUC60>2.5}$) were calculated by dividing the enhancing volume (volume of voxels with $IAUC_{60}$ > 0 mMol.s for $EnF_{IAUC60>0}$ and volume of voxels with $IAUC_{60}$ > 2.5 mMol.s for $EnF_{IAUC60>2.5}$) by the total volume of the tumour VOI. The cut off threshold of $IAUC_{60}$ > 2.5 mMol.s for $EnF_{IAUC60>2.5}$ was previously identified as a optimal threshold for allowing the distinction of high from low grade glioma (40).

Histopathological data analysis

Two experienced neuropathologists (DDP and PP) performed the histopathological analysis. Histological specimens were assessed for the following: necrosis (presence or absence of frank and/or geographic necrosis), cell density (3 point grading score), cell atypia (3 point grading score), mitotic activity (number of mitotic figures seen per 10 high power field units), infiltrates (presence or absence of lymphocytes and/or macrophages), tumour vascular pattern (presence or absence of the following features; endothelial hypertrophy and/or hyperplasia, glomeruloid structures, granulation tissue, large vessel density, thrombosis, sclerosed vessels), an overall vascular density score (3 point grading score) and histological pattern (fibrillar, gemistocytic, oligodendrocytes, sarcomatous, giant cells and small cells) in conjunction with standard histopathological subtyping and grading according to the WHO classification criteria (1). Vascular and histological features were not mutually exclusive, therefore more than one feature could be described in a given tumour specimen.

Quantitative measurement of the endothelial surface area (ESA), the vascular surface area (VSA) and the vascular profile count per mm^2 (VPC) was made using CD34 immunostaining and dedicated image analysis software.

Statistical analysis

Statistical analysis was performed using SPSS (version 15.0, SPSS Inc., Chicago, USA) nonparametric statistical tests. Where histological parameters produce a binary classification (necrosis, infiltrates, vascular patterns and histological patterns) Mann Whitney U tests were performed to test the hypothesis that MRI parameter values did not differ between groups. Where histological features produce categorical scores (cell density, cell atypia and overall vascular score) multivariate analysis of variance (ANOVA) was used to test the hypotheses that MRI parameter values did not differ between groups. Spearman's correlation analysis was performed to assess the relationship between quantitative histological measures (mitotic activity, ESA, VSA and VPC) and MRI parameters and to identify correlation between the individual MRI measurements. For Mann Whitney U and ANOVA testing a result was considered to be significantly different if $p<0.01$, given the number of variables assessed. For Spearman's correlation analysis significance was taken as <0.05.

Results

28 untreated newly presently GBM were included in the study (10 female, age range 38 - 76 years, mean 60 years). Histological specimens were obtained from 12 biopsies and 16 surgical debulkings. Results of statistical analyses for comparisons of histological and MRI measures are summarized in Table 1.

The presence of frank necrosis was associated with significantly higher values of K^{trans} ($p<0.01$, Figure 1). Significantly higher values of v_e were seen in the presence fibrillary histology (estimated $p<0.01$, Figure 1). A positive correlation was found between v_e and mitotic activity ($p<0.05$, $\rho = 0.470$, Figure 2). No relationship was seen between mitotic activity and any of the descriptive or semi-quantitative histology measures, suggesting the relationship between v_e and mitotic activity is independent of the relationship between v_e

and the presence of fibrillar histology. No correlation was observed between v_e and cell density.

Cross correlations between individual MRI parameters are summarised in Table 2. Positive correlations were found between K^{trans} and all other MRI parameters. Significant correlations were present between v_e and K^{trans} ($p<0.05$ and $\rho=0.450$) and between v_p and EnF. Mitotic activity did not correlate with any quantitative vascular measure, but cross correlation was seen across all three histological vascular metrics (Table 3). No other significant relationships were identified between histological measures.

Discussion

Whilst there has been considerable interest in the development of imaging biomarkers for use in clinical trials, the majority of DCE-MRI studies have focused on identifying correlates of vascularity and angiogenesis (41). This study identified an unexpected positive correlation between v_e, a parameter thought to reflect EES volume, and mitotic activity. No relationships were identified between previously described DCE-MRI prognosticators, K^{trans} and v_p, and mitotic activity, nor between vascular patterns and DCE-MRI measures.

The parameter v_e is often overlooked in DCE-MRI studies. In cerebral tumours, it has potential to distinguish intra- from extra-axial tumours (42,43), and exhibits increased values with increasing tumour grade (33,34,42,44). It has also demonstrated sensitivity in identifying changes in response to treatment with corticosteroids, with decreases in v_e, presumably reflecting a reduction in interstitial oedema (45,46). In a study of vestibular schwannomas, meningiomas and gliomas, no direct measure of the EES or cell density measure was made but v_e values in schwannoma were noted to be significantly larger than in glioma, where cell density is higher (43). In a study comparing v_e with ADC in glioma, no relationship was found between the two metrics suggesting that these parameters may provide independent information about the extravascular extracellular space (35). This may reflect the existence of separate extravascular leakage compartments characterised by fast and contrast agent exchange, possibly reflecting the presence of slow leakage / diffusion into and out of necrotic tumour spaces (42,47,48). Previous studies have also reported correlations between MVD and both v_e and K^{trans} (33,34). We did not find this correlation in our study but there was a cross correlation between the DCE-MRI parameters v_e and K^{trans} and raising the possibility that the correlation reported in the previous studies reflects the relationship of v_e with K^{trans} rather than MVD. A previous rat xenograft study has reported correlation between v_e and cellular density (36), but our current study found no such relationship. Histological measures of cell density are often a count of the number of cell nuclei per unit area and without quantification of the amount of tissue the cells occupy, thus an increase in histological cell density may reflect an increase in number of cells, but not necessarily a decrease in extra-vascular, extra cellular space if the cells are small in size. It should be noted that there are potential modelling problems associated with the calculation of v_e. Clearly it can be estimated only in perfused tissue where there is significant leakage of contrast agent (35). This means that summary statistics presented in this and other studies reflect only perfused tissue with contrast agent leakage, in contrast to diffusion-weighted imaging where high ADC values are seen in association with necrosis. We have specifically

excluded non-perfusing tissue from estimates of summary statistics, which could otherwise produce artificially low values of v_e. In addition, the relatively low dynamic sampling duration (6 minutes) will affect v_e estimates to some degree. First, model fitting errors (assuming the model is correct) will result from undersampling, but modelling studies suggest that these fitting errors are likely to be very small (49). Second, short sampling times will lead to relative under-representation of slow tissue exchange compartments, which would tend to reduce the impact of necrotic tissue on v_e estimations as described in (42,47,48). This implies that tumours with greater necrosis would have shown higher v_e values if sampling had continued for a longer time and that the measured values of v_e in this study are more likely to reflect EES fraction in viable tissue.

The positive correlation between v_e and mitotic activity is surprising. Tumours with larger v_e values exhibited more mitotic activity, the inverse of what one might expect (and the inverse of our initial hypothesis), whereby more proliferative tumours would be more densely packed with cells. Neither mitotic activity nor v_e related to the presence of necrosis, although the lack of relationship between v_e and necrosis may in part reflect the relatively low dynamic collection period (*vide supra*). These observations suggest that the size of the EES in perfused enhancing tumour tissue is truly related to mitotic rate and not simply a reflection of elevated measures of v_e due to increased necrosis in rapidly proliferating tumours.

This is initially counter-intuitive. It is well known that in normal developing tissues mitotic activity is higher in areas of low cell packing due to inhibition of proliferation in response to cell to cell contact, a process known as contact inhibition of proliferation (CIP) in developing normal tissue (50). No similar relationship has been described in malignant tissues and loss of contact inhibition of mitosis is one of the hallmarks of the cancer cell (51). This leads to the hypothesis, stated in the introduction, that rapidly proliferating tumours will continue to proliferate leading to increased cell density and decreased size of the EES and consequently of v_e. We have no evidence to explain why the observed relationship should exist. One possible explanation may be that tumours with high cellular density still have impaired responses to tumoural growth factors despite loss of CIP (52). Another possible explanation is that tumours with short mitotic cycles are characterised by reduced time for cellular maturation resulting in smaller cells and reduced cell packing. Whatever the underlying biological mechanism this finding appears particularly interesting and requires further study.

The ability to obtain an MRI-based imaging biomarker of mitotic activity and/or tumour cell proliferation is highly desirable. The findings presented here may be tumour specific or reflect an unrecognised phenotype, but the possibility that v_e may be a potential marker of mitotic activity merits further evaluation.

The data also demonstrated a positive relationship between tumour cell fibrillarity within the histological specimens and higher v_e, although the numbers were very small (n=4). Fibrillar cell processes are cell extensions containing cytoplasm, which are surrounded by cell membranes. These are visible through a microscope and allow tumour astrocytes to be recognised as “fibrillar”. A less cell-dense arrangement due to such cell extensions and/or

intercellular oedema facilitate its recognition via light microscopy. Thus, the ability to identify fibrillar cell processes suggests that the tumour cells are more loosely packed or there is localized extracellular oedema. No relationship was identified between fibrillar histology and mitotic activity indicating that the relationships between v_e and these measures are independent.

The majority of previous work evaluating the relationship between specific histological features and DCE-MRI has focused predominantly on CBV derived from DSC techniques with significant relationships seen between CBV and MVD (26-29), VEGF expression (27,30), cell density (29), endothelial proliferation (31) and mitotic activity (31). No such relationships were identified between these latter three measures and v_p in this study. A study by Ludemann et al compared a variety of MR imaging techniques with $H_2{}^{15}O$-PET for measuring perfusion (53) and found that whilst both DSC and T_1-weighted DCE-MRI techniques correlated with the gold standard $H_2{}^{15}O$-PET measure, only borderline correlation was seen between the DSC techniques and the T_1-weighted technique, whereby DSC derived blood volumes were generally lower than those derived from the T_1-weighted DCE-MRI technique. This may account for the failure of v_p to relate to any of the histological measures in this study.

The major limitation of the present work is the lack of stereotactic image matched histological specimens and therefore correlation between the histology and the DCE-MRI measurements at a local level cannot be made. GBMs are notoriously heterogeneous tumours and histological analysis of small tumour specimens may lead to under-grading of a tumour if the sample is not a true reflection of the tumour as a whole. At the time of the study, imaged matched histological samples were not obtained and there was no concurrent post-operative imaging performed which could have helped to identify the site of the histological sample. All histological specimens in this study did confirm the diagnosis of GBM and therefore are considered representative samples. Previous non image registered studies comparing v_e with histopathological vascular measures have been reported but these have been performed with a selection of 3-4 small ROIs, taking the maximal value of v_e and K^{trans} (33,34), which is unlikely to provide a representation of the tumour as a whole. In our current study, for the DCE-MRI measures K^{trans}, v_e, and v_p, median values from whole tumour VOIs were used. Studies using whole tumour VOIs have previously identified significant differences in DCE-MRI parameters between tumour grades (17), and been shown to convey important potential prognostic information (25). Thus a comparison between small histological samples and DCE-MRI parameters from whole tumour VOIs seems reasonable. Further work is required to confirm that the correlations identified in this current study hold true for image matched stereotactic samples. In addition, some histological features such as Ki-67 and VEGF expression, which have previously shown correlation with DSC-MRI derived CBV (20,26-30), were not available.

Conclusion

The DCE-MRI derived measure, v_e, has been identified as a potential correlate of mitotic activity in GBM. Whilst this is an interesting result, our understanding of the biological mechanisms responsible for this possible relationship is limited. Further work with the

correlation of v_e to more precise measures of cell density, additional markers of cellular and vascular proliferation, and measures of VEGF expression is warranted.

Acknowledgments

Funding

This works was funded as part of a CRUK Clinical Research Training Fellowship, ref: C21247/A7473.

Abbreviations

DCE-MRI	dynamic contrast enhanced MRI
EES	extravascular extracellular space
EnF	enhancing fraction
ESA	endothelial surface area
^{18}F-FLT	^{18}F-labeled 3′-deoxy-3′-fluorothymidine
GBM	glioblastoma multiforme
$IAUC_{60}$	initial area under the contrast agent concentration curve
K^{trans}	contrast transfer coefficient
MVD	microvascular density
v_e	volume of the EES per unit tissue volume
VEGF	vascular endothelial growth factor
v_p	volume of the blood plasma per unit tissue volume
VPC	vascular profile count per mm^2 (VPC)
VSA	vascular surface area
WHO	World Health Organisation

References

1. Louis DN, Ohgaki H, Wiestler OD, et al. The 2007 WHO Classification of Tumours of the Central Nervous System. Acta Neuropathol. 2007; 1142:97–109. [PubMed: 17618441]
2. Struikmans H, Rutgers DH, Jansen GH, et al. Prognostic relevance of MIB-1 immunoreactivity, S-phase fraction, 5-bromo-2′-deoxyuridine labeling indices, and mitotic figures in gliomas. Radiat Oncol Investig. 1999; 74:243–48.
3. Korshunov A, Golanov A, Sycheva R. Immunohistochemical markers for prognosis of anaplastic astrocytomas. J. Neurooncol. 2002; 583:203–15. [PubMed: 12187956]
4. Scott JN, Rewcastle NB, Brasher PM, et al. Which glioblastoma multiforme patient will become a long-term survivor? A population-based study. Ann. Neurol. 1999; 462:183–88. [PubMed: 10443883]

5. Abdulrauf SI, Edvardsen K, Ho KL, et al. Vascular endothelial growth factor expression and vascular density as prognostic markers of survival in patients with low-grade astrocytoma. J. Neurosurg. 1998; 883:513–20. [PubMed: 9488306]
6. Yao Y, Kubota T, Takeuchi H, et al. Prognostic significance of microvessel density determined by an anti-CD105/endoglin monoclonal antibody in astrocytic tumors: comparison with an anti-CD31 monoclonal antibody. Neuropathology. 2005; 253:201–6. [PubMed: 16193836]
7. Preusser M, Gelpi E, Matej R, et al. No prognostic impact of survivin expression in glioblastoma. Acta Neuropathol. 2005; 1095:534–38. [PubMed: 15843906]
8. Birner P, Piribauer M, Fischer I, et al. Vascular patterns in glioblastoma influence clinical outcome and associate with variable expression of angiogenic proteins: evidence for distinct angiogenic subtypes. Brain Pathol. 2003; 132:133–43. [PubMed: 12744467]
9. Colman H, Giannini C, Huang L, et al. Assessment and prognostic significance of mitotic index using the mitosis marker phospho-histone H3 in low and intermediate-grade infiltrating astrocytomas. Am. J. Surg. Pathol. 2006; 305:657–64. [PubMed: 16699322]
10. Coleman KE, Brat DJ, Cotsonis GA, et al. Proliferation (MIB-1 expression) in oligodendrogliomas: assessment of quantitative methods and prognostic significance. Appl. Immunohistochem. Mol. Morphol. 2006; 141:109–14. [PubMed: 16540741]
11. Flynn JR, Wang L, Gillespie DL, et al. Hypoxia-regulated protein expression, patient characteristics, and preoperative imaging as predictors of survival in adults with glioblastoma multiforme. Cancer. 2008; 1135:1032–42. [PubMed: 18618497]
12. Karayan-Tapon L, Wager M, Guilhot J, et al. Semaphorin, neuropilin and VEGF expression in glial tumours: SEMA3G, a prognostic marker? Br. J. Cancer. 2008; 997:1153–60. [PubMed: 18781179]
13. Nam D-H, Park K, Suh YL, et al. Expression of VEGF and brain specific angiogenesis inhibitor-1 in glioblastoma: prognostic significance. Oncol. Rep. 2004; 114:863–69. [PubMed: 15010886]
14. Oehring RD, Miletic M, Valter MM, et al. Vascular endothelial growth factor (VEGF) in astrocytic gliomas--a prognostic factor? J. Neurooncol. 1999; 452:117–25. [PubMed: 10778727]
15. Tofts PS. Modeling tracer kinetics in dynamic Gd-DTPA MR imaging. J. Magn. Reson. Imaging. 1997; 71:91–101. [PubMed: 9039598]
16. Law M, Yang S, Wang H, et al. Glioma grading: sensitivity, specificity, and predictive values of perfusion MR imaging and proton MR spectroscopic imaging compared with conventional MR imaging. AJNR Am J Neuroradiol. 2003; 2410:1989–98. [PubMed: 14625221]
17. Patankar TF, Haroon HA, Mills SJ, et al. Is volume transfer coefficient (K(trans)) related to histologic grade in human gliomas? AJNR Am J Neuroradiol. 2005; 2610:2455–65. [PubMed: 16286385]
18. Sugahara T, Korogi Y, Kochi M, et al. Correlation of MR imaging-determined cerebral blood volume maps with histologic and angiographic determination of vascularity of gliomas. AJR Am J Roentgenol. 1998; 1716:1479–86. [PubMed: 9843274]
19. Roberts HC, Roberts TP, Brasch RC, et al. Quantitative measurement of microvascular permeability in human brain tumors achieved using dynamic contrast-enhanced MR imaging: correlation with histologic grade. AJNR Am J Neuroradiol. 2000; 215:891–99. [PubMed: 10815665]
20. Roberts HC, Roberts TP, Bollen AW, et al. Correlation of microvascular permeability derived from dynamic contrast-enhanced MR imaging with histologic grade and tumor labeling index: a study in human brain tumors. Acad Radiol. 2001; 85:384–91. [PubMed: 11345268]
21. Law M, Young R, Babb J, et al. Comparing perfusion metrics obtained from a single compartment versus pharmacokinetic modeling methods using dynamic susceptibility contrast-enhanced perfusion MR imaging with glioma grade. AJNR Am J Neuroradiol. 2006; 279:1975–82. [PubMed: 17032878]
22. Lev MH, Ozsunar Y, Henson JW, et al. Glial tumor grading and outcome prediction using dynamic spin-echo MR susceptibility mapping compared with conventional contrast-enhanced MR: confounding effect of elevated rCBV of oligodendrogliomas [corrected]. AJNR Am J Neuroradiol. 2004; 252:214–21. [PubMed: 14970020]

23. Law M, Young RJ, Babb JS, et al. Gliomas: predicting time to progression or survival with cerebral blood volume measurements at dynamic susceptibility-weighted contrast-enhanced perfusion MR imaging. Radiology. 2008; 2472:490–98. [PubMed: 18349315]
24. Cao Y, Tsien CI, Nagesh V, et al. Survival prediction in high-grade gliomas by MRI perfusion before and during early stage of RT [corrected]. Int. J. Radiat. Oncol. Biol. Phys. 2006; 643:876–85. [PubMed: 16298499]
25. Mills SJ, Patankar TA, Haroon HA, et al. Do cerebral blood volume and contrast transfer coefficient predict prognosis in human glioma? AJNR Am J Neuroradiol. 2006; 274:853–58. [PubMed: 16611778]
26. Cha S, Johnson G, Wadghiri YZ, et al. Dynamic, contrast-enhanced perfusion MRI in mouse gliomas: correlation with histopathology. Magn. Reson. Med. 2003; 495:848–55. [PubMed: 12704767]
27. Haris M, Husain N, Singh A, et al. Dynamic contrast-enhanced derived cerebral blood volume correlates better with leak correction than with no correction for vascular endothelial growth factor, microvascular density, and grading of astrocytoma. J Comput Assist Tomogr. 2008; 326:955–65. [PubMed: 19204461]
28. Liao W, Liu Y, Wang X, et al. Differentiation of primary central nervous system lymphoma and high-grade glioma with dynamic susceptibility contrast-enhanced perfusion magnetic resonance imaging. Acta Radiol. 2009; 502:217–25. [PubMed: 19096950]
29. Sadeghi N, D'Haene N, Decaestecker C, et al. Apparent diffusion coefficient and cerebral blood volume in brain gliomas: relation to tumor cell density and tumor microvessel density based on stereotactic biopsies. AJNR Am J Neuroradiol. 2008; 293:476–82. [PubMed: 18079184]
30. Maia ACM, Malheiros SMF, da Rocha AJ, et al. MR cerebral blood volume maps correlated with vascular endothelial growth factor expression and tumor grade in nonenhancing gliomas. AJNR Am J Neuroradiol. 2005; 264:777–83. [PubMed: 15814920]
31. Sadeghi N, Salmon I, Decaestecker C, et al. Stereotactic comparison among cerebral blood volume, methionine uptake, and histopathology in brain glioma. AJNR Am J Neuroradiol. 2007; 283:455–61. [PubMed: 17353312]
32. Callot V, Galanaud D, Figarella-Branger D, et al. Correlations between MR and endothelial hyperplasia in low-grade gliomas. J. Magn. Reson. Imaging. 2007; 261:52–60. [PubMed: 17659539]
33. Jia ZZ, Gu HM, Zhou XJ, et al. The assessment of immature microvascular density in brain gliomas with dynamic contrast-enhanced magnetic resonance imaging. Eur J Radiol. 2015; 849:1805–9. [PubMed: 26066470]
34. Li X, Zhu Y, Kang H, et al. Glioma grading by microvascular permeability parameters derived from dynamic contrast-enhanced MRI and intratumoral susceptibility signal on susceptibility weighted imaging. Cancer Imaging. 2015; 151:4. [PubMed: 25889239]
35. Mills SJ, Soh C, Rose CJ, et al. Candidate biomarkers of extravascular extracellular space: a direct comparison of apparent diffusion coefficient and dynamic contrast-enhanced MR imaging--derived measurement of the volume of the extravascular extracellular space in glioblastoma multiforme. AJNR Am J Neuroradiol. 2010; 313:549–53. [PubMed: 19850765]
36. Aryal MP, Nagaraja TN, Keenan KA, et al. Dynamic contrast enhanced MRI parameters and tumor cellularity in a rat model of cerebral glioma at 7 T. Magn. Reson. Med. 2014; 716:2206–14. [PubMed: 23878070]
37. Bastin ME, Carpenter TK, Armitage PA, et al. Effects of dexamethasone on cerebral perfusion and water diffusion in patients with high-grade glioma. AJNR Am J Neuroradiol. 2006; 272:402–8. [PubMed: 16484419]
38. Thompson, G.; Cain, J.; Jackson, A., et al. Interobserver agreement for cerebral glioma volumetrics on conventional MR imaging. Conference Proceedings of the 16th Annual Meeting of ISMRM; 2008;
39. Parker, GJ.; Jackson, A.; Waterton, JC. Automated arterial input function extraction for T1-weighted DCE-MRI. Conference Proceedings of the 11th Annual Meeting of ISMRM; 2003.
40. Mills SJ, Soh C, O'Connor JPB, et al. Tumour enhancing fraction (EnF) in glioma: relationship to tumour grade. Eur Radiol. 2009; 196:1489–98. [PubMed: 19198847]

41. O'Connor JPB, Jackson A, Parker GJM, et al. DCE-MRI biomarkers in the clinical evaluation of antiangiogenic and vascular disrupting agents. Br. J. Cancer. 2007; 962:189–95. [PubMed: 17211479]

42. Lüdemann L, Grieger W, Wurm R, et al. Quantitative measurement of leakage volume and permeability in gliomas, meningiomas and brain metastases with dynamic contrast-enhanced MRI. Magnetic Resonance Imaging. 2005; 238:833–41. [PubMed: 16275421]

43. Zhu XP, Li KL, Kamaly-Asl ID, et al. Quantification of endothelial permeability, leakage space, and blood volume in brain tumors using combined T1 and T2* contrast-enhanced dynamic MR imaging. J. Magn. Reson. Imaging. 2000; 116:575–85. [PubMed: 10862055]

44. Lüdemann L, Grieger W, Wurm R, et al. Comparison of dynamic contrast-enhanced MRI with WHO tumor grading for gliomas. Eur Radiol. 2001; 117:1231–41. [PubMed: 11471617]

45. Andersen C, Jensen FT. Differences in blood-tumour-barrier leakage of human intracranial tumours: quantitative monitoring of vasogenic oedema and its response to glucocorticoid treatment. Acta Neurochir (Wien). 1998; 1409:919–24. [PubMed: 9842429]

46. Armitage PA, Schwindack C, Bastin ME, et al. Quantitative assessment of intracranial tumor response to dexamethasone using diffusion, perfusion and permeability magnetic resonance imaging. Magnetic Resonance Imaging. 2007; 253:303–10. [PubMed: 17371718]

47. Fluckiger JU, Loveless ME, Barnes SL, et al. A diffusion-compensated model for the analysis of DCE-MRI data: theory, simulations and experimental results. Phys. Med. Biol. 2013; 586:1983–98. [PubMed: 23458745]

48. Lüdemann L, Hamm B, Zimmer C. Pharmacokinetic analysis of glioma compartments with dynamic Gd-DTPA-enhanced magnetic resonance imaging. Magnetic Resonance Imaging. 2000; 1810:1201–14. [PubMed: 11167040]

49. Cheng H-LM. Investigation and optimization of parameter accuracy in dynamic contrast-enhanced MRI. J. Magn. Reson. Imaging. 2008; 283:736–43. [PubMed: 18777534]

50. McClatchey AI, Yap AS. Contact inhibition (of proliferation) redux. Current Opinion in Cell Biology. 2012; 245:685–94. [PubMed: 22835462]

51. Tumanishvili GD, Salamatina NV. Action of nuclear and cytoplasmic fractions of liver homogenate on liver growth in the chick embryo. J Embryol Exp Morphol. 1968; 201:53–71. [PubMed: 5693889]

52. Mayor R, Carmona-Fontaine C. Keeping in touch with contact inhibition of locomotion. Trends in Cell Biology. 2010; 206:319–28. [PubMed: 20399659]

53. Lüdemann L, Warmuth C, Plotkin M, et al. Brain tumor perfusion: comparison of dynamic contrast enhanced magnetic resonance imaging using T1, T2, and T2* contrast, pulsed arterial spin labeling, and H2(15)O positron emission tomography. Eur J Radiol. 2009; 703:465–74. [PubMed: 18359598]

Europe PMC Funders Author Manuscripts

Europe PMC Funders Author Manuscripts

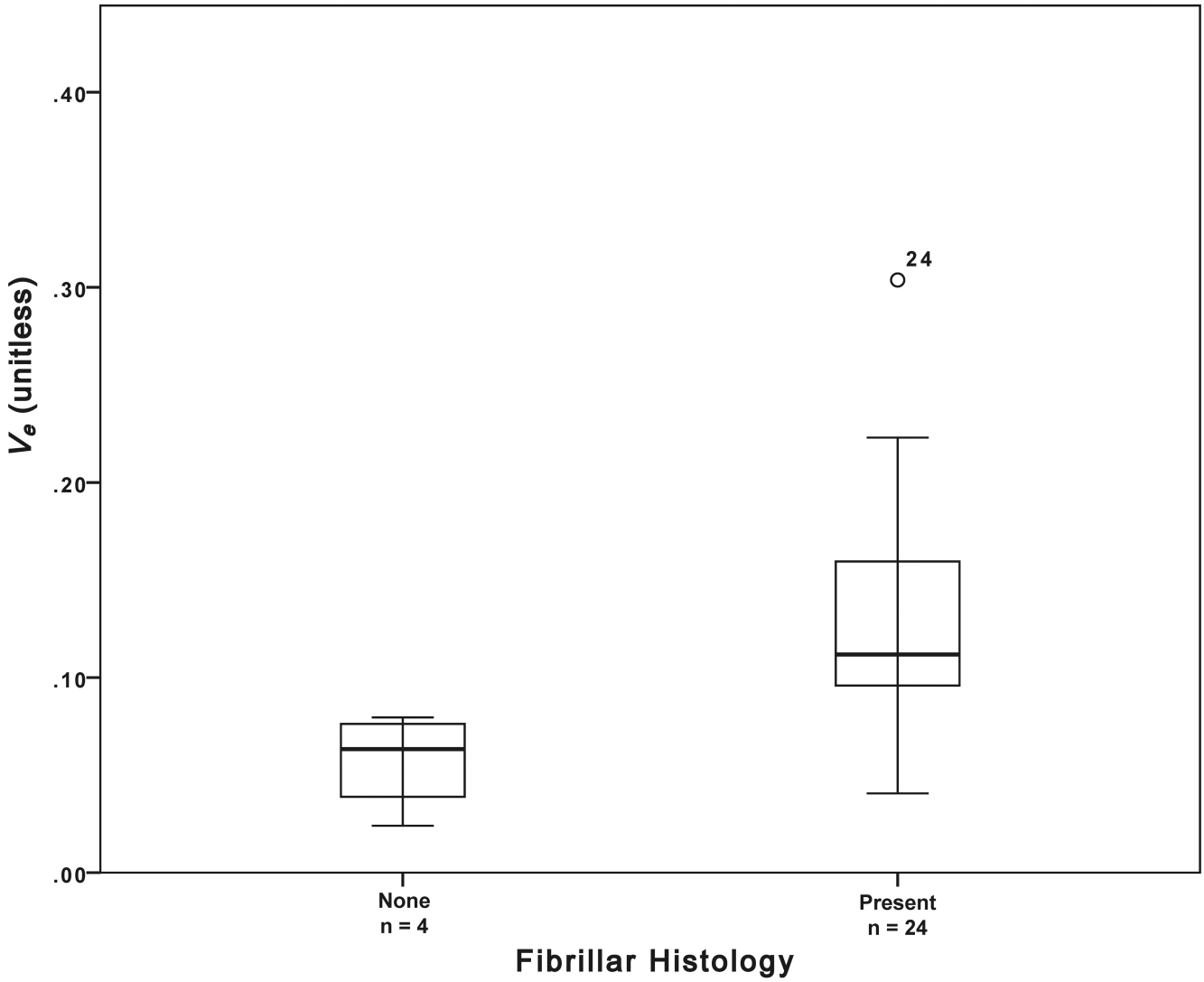

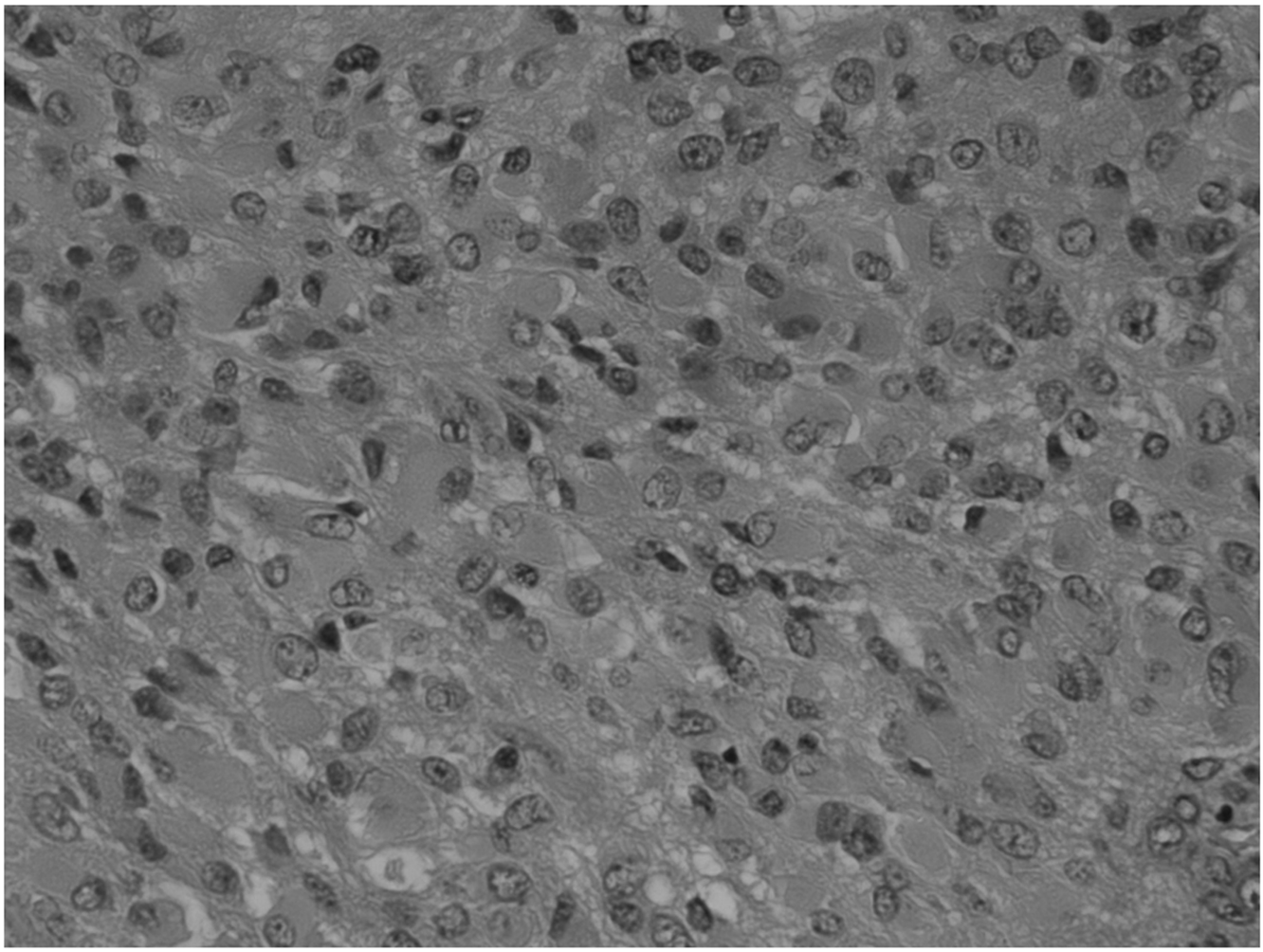

Europe PMC Funders Author Manuscripts

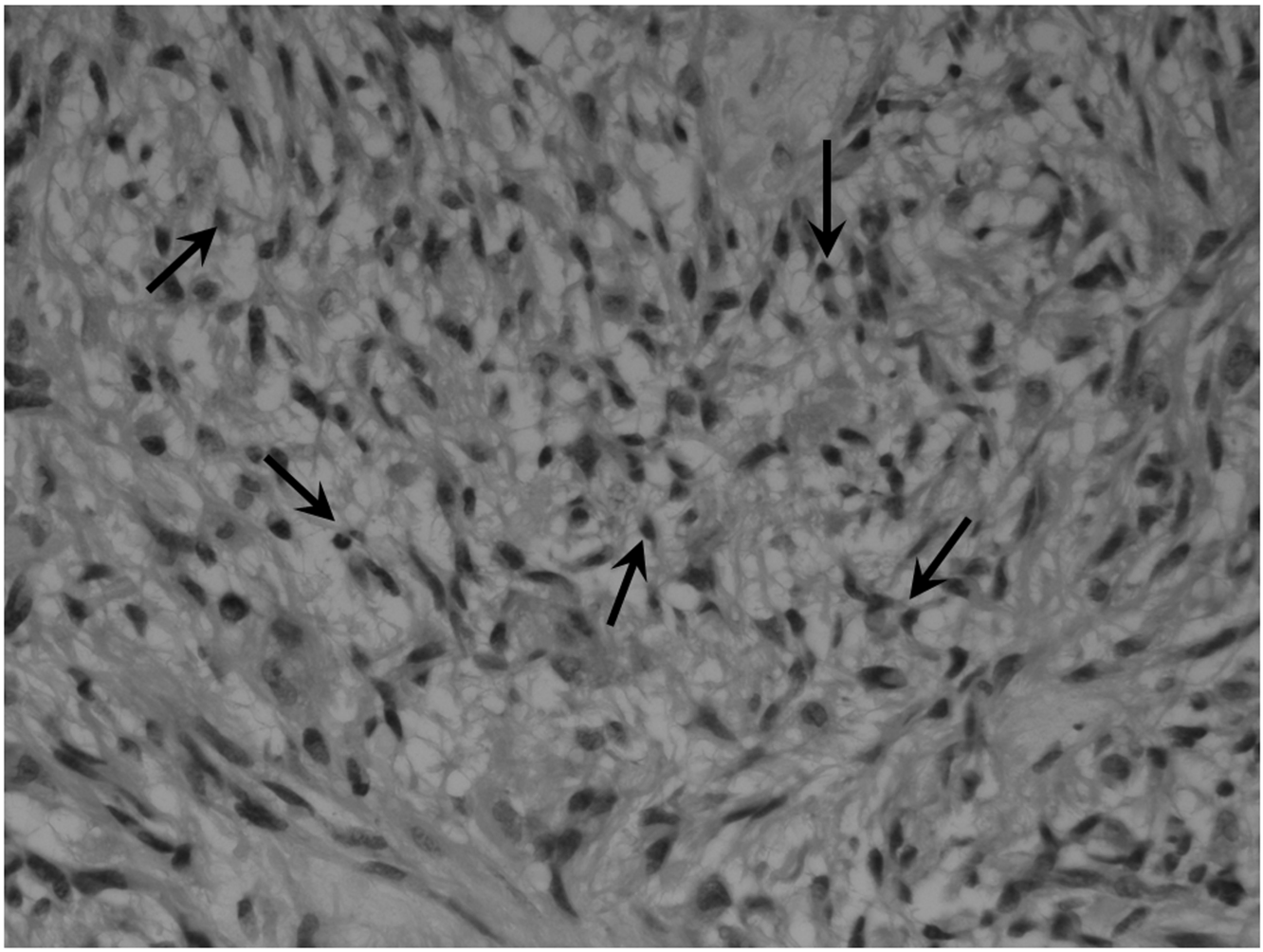

Europe PMC Funders Author Manuscripts

Europe PMC Funders Author Manuscripts

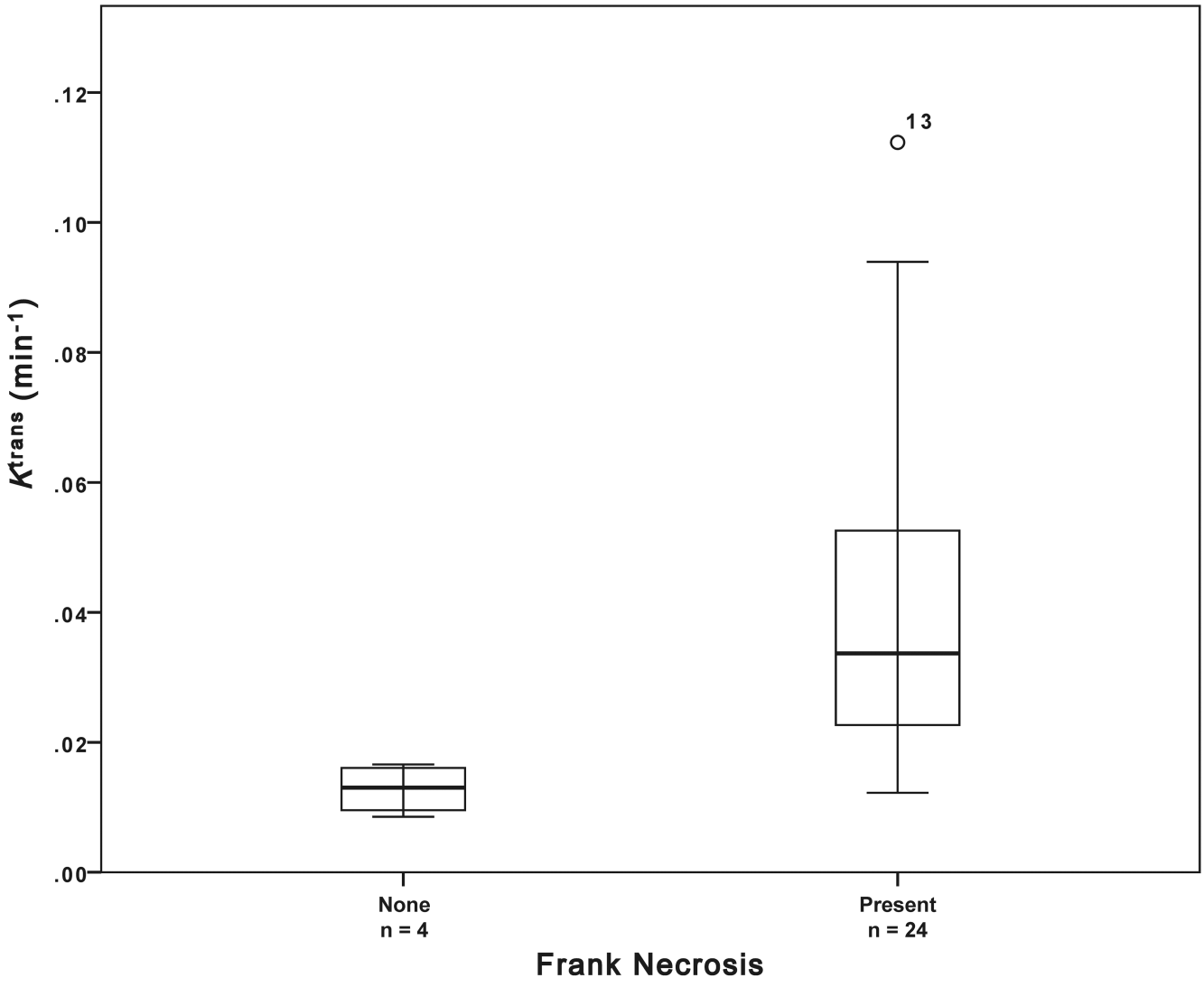

Figure 1.

a) Boxplot of fibrillar histology and ve (estimated p = 0.007). b) Example histological specimens showing tumours without and c) with the presence of fibrils (small fibres measuring approximately 1 mm, black arrows). H&E stain × 40 magnification. d) Boxplot of frank necrosis and Ktrans (estimated p = 0.005).

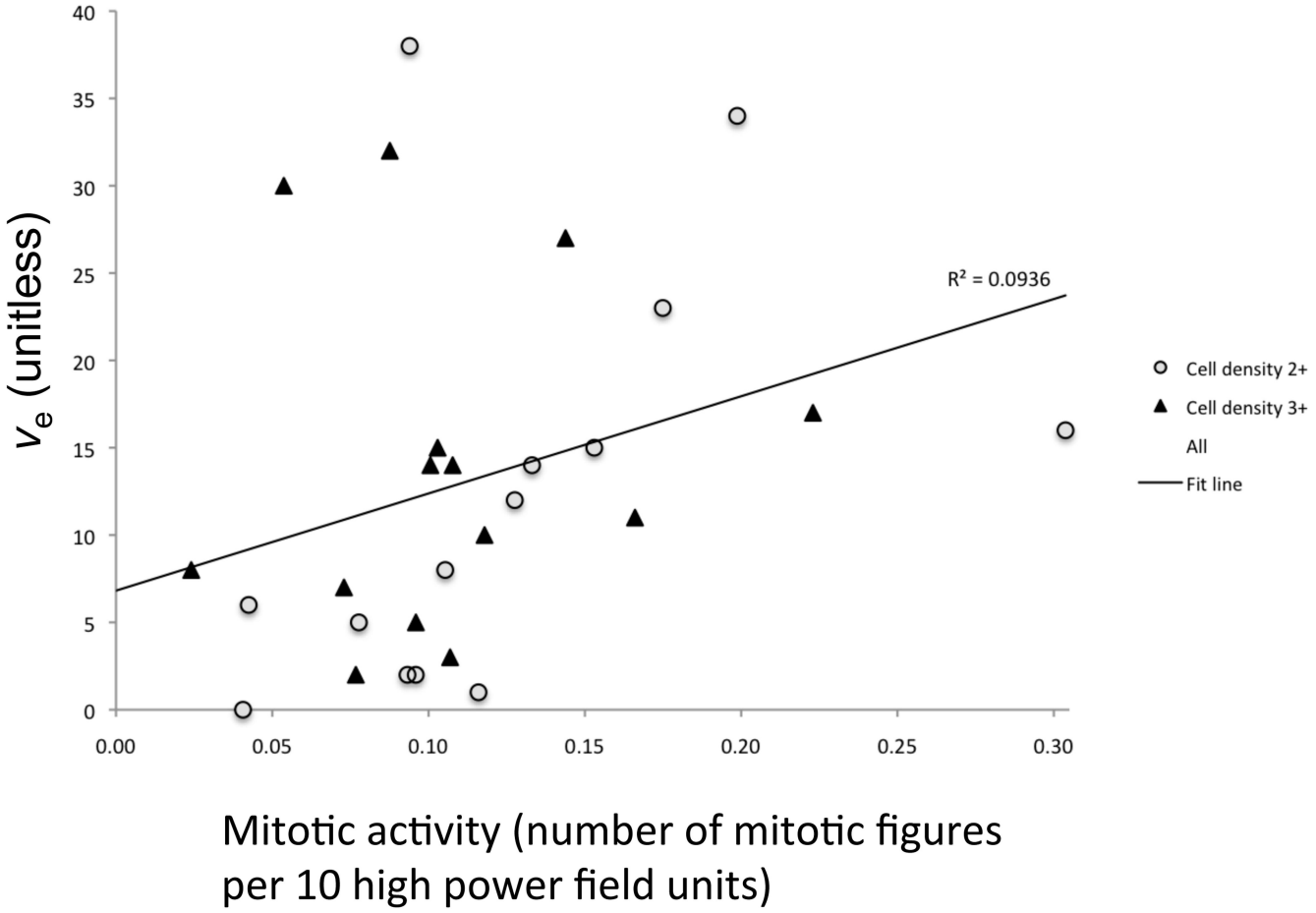

Figure 2.
Scatter plot of mitotic activity versus ve (p = 0.012, r = 0.470), colour coded to demonstrate separate scores of cell density measures.

Table 1

Summary of statistical comparisons between histopathological and DCE-MRI measures. Mann Whitney U tests were used for histological parameters which produce a binary classification (necrosis, infiltrates, vascular patterns and histological patterns) and multivariate analysis of variance (ANOVA) was used for histological features which produce categorical scores (cell density, cell atypia and overall vascular score). Spearman's correlation analysis was performed to assess the relationship between MR derived parameters and quantitative histological measures (mitotic activity, ESA, VSA and VPC). Significance levels are shown and Spearman's ρ is shown for correlation analyses.

Histo-Pathological Feature \ MRI Measure		K^{trans} (min^{-1})	v_e (unitless)	v_p (unitless)	$EnF_{IAUC60>0}$ (unitless)	$EnF_{IAUC60>2.5}$ (unitless)
Necrosis	Frank	0.005 **	0.694	0.694	0.264	0.088
	Geographic	0.495	0.655	0.466	0.384	0.796
Cell density		0.392	0.165	0.953	0.455	0.169
Cell atypia		0.958	0.629	0.654	0.630	0.149
Mitotic activity		0.400 ρ=0.166	0.012 * ρ=0.470	0.678 ρ=−0.082	0.729 ρ=−0.069	0.744 ρ=0.065
Infiltrates	Lymphocytes	0.353	0.147	0.911	0.629	0.393
	Macrophages	0.629	0.738	0.683	0.629	0.970
Tumour vascular patterns	Hypertrophy	0.592	0.592	0.153	0.422	0.212
	Hyperplasia	0.569	0.787	0.197	0.787	0.418
	Glomeruloid	0.394	0.504	0.504	0.134	0.596
	Granulation tissue	0.325	0.896	0.896	0.015	0.076
	Large vessel	0.164	0.164	0.137	0.848	0.502
	Thrombosis	0.472	0.924	0.632	0.472	0.811
	Sclerosed	0.293	0.095	0.155	0.951	0.122
Histological patterns	Fibrillar	0.325	0.007 **	0.325	0.793	0.212
	Gemistocytic	0.937	0.442	0.614	0.730	0.353
	Oligodendro	0.155	0.353	0.757	0.155	0.155
	Sarcomatous	0.929	0.789	0.929	0.372	0.592
	Giant Cells	0.697	0.697	0.976	0.787	0.610
	Small Cells	0.970	0.683	0.911	0.738	0.738
Overall vascular score		0.125	0.759	0.385	0.214	0.278
Vascular measures	ESA Ratio	0.839 ρ=0.041	0.809 ρ=−0.049	0.493 ρ=−0.0138	0.344 ρ=−0.189	0.799 ρ=−0.051
	VSA Ratio	0.919 ρ=0.020	0.855 ρ=−0.037	0.495 ρ=−0.137	0.298 ρ=−0.208	0.782 ρ=−0.056
	VPCmm^{-2}	0.224 ρ=0.242	0.626 ρ=−0.098	0.119 ρ=0.307	0.065 ρ=0.360	0.071 ρ=0.353

* significance taken as $p < 0.05$ (Spearman's correlation analysis)

** significance taken as $p < 0.01$(Mann Whitney U and ANOVA)

Europe PMC Funders Author Manuscripts

Table 2

Cross correlations of MRI parameters. Significance levels and Spearman's ρ are shown.

	Untreated GBM (n = 28)			
	v_e	**v_p**	**$EnF_{IAUC60>0}$**	**$EnF_{IAUC60>2.5}$**
K^{trans}	0.016 * ρ=0.450	0.006 ** ρ=0.507	0.005 ** ρ=0.513	<0.001 ** ρ=0.784
v_e		0.105 ρ=0.313	0.888 ρ=0.028	0.059 ρ=0.361
v_p			0.02 * ρ=0.437	<0.001 ** ρ=0.620
$EnF_{IAUC60>0}$				<0.001 ** ρ=0.825

* significance taken as $p < 0.05$

** significance taken as $p < 0.01$

Europe PMC Funders Author Manuscripts

Table 3

Cross correlations of quantitative histological measures. Significance levels and Spearman's ρ are shown.

	Untreated GBM (n = 28)		
	ESA ratio	**VSA ratio**	**VPC/mm^2**
Mitotic activity	0.098 ρ=0.325	0.066 ρ=0.358	0.737 ρ=0.068
ESA ratio		<0.001 ** ρ=0.993	0.04 * ρ=0.530
VSA ratio			0.04 * ρ=0.532

* significance taken as $p < 0.05$

** significance taken as $p < 0.01$